OPEN

NPG Asia Materials (2015) 7, e174; doi:10.1038/am.2015.28

www.nature.com/am

ORIGINAL ARTICLE

POSS ionic liquid crystals

Kazuo Tanaka, Fumiyasu Ishiguro, Jong-Hwan Jeon, Tatsuhiro Hiraoka and Yoshiki Chujo

Here we report the use of unique organic – inorganic hybrid materials composed of octa-substituted polyhedral oligomeric silsesquioxane (POSS) cores as ionic liquid (IL) crystals. These materials have a wide temperature range in which they exist in liquid crystal (LC) phase because of the stabilizing effect of the POSS core. We synthesized ion pairs composed of alkyl chain-substituted imidazolium and carboxylates of various lengths that were or were not connected to the POSS core; then the thermal properties of these materials were investigated. It was found that both ion salts and the octadecyl-substituted imidazolium ion pairs with or without connection to POSS could form LCs. Interestingly, the LC phase of the POSS-tethered ion salts was maintained until decomposition. In contrast, the octadecyl-substituted imidazolium ion salts that were not tethered to the POSS core showed a clearance point during heating. The highly symmetric structure of POSS contributes not only to the suppression of the molecular motion of the ion salts, but also results in the formation of regular structures, leading to thermally stable, thermotropic IL crystals.
NPG Asia Materials (2015) **7,** e174; doi:10.1038/am.2015.28; published online 17 April 2015

INTRODUCTION

Ionic liquid (IL) crystals are highly relevant and are being heavily researched. The unique characteristics, especially their novel optical properties, of liquid crystals (LCs) have been reported previously.[1,2] In addition, by using electrostatic interactions originating among ionic moieties, robust chiral structures can be produced.[3,4] Even a small quantity of chiral ionic sources can efficiently induce enantiomeric structures in a bulk sample, and ionic moieties can be assembled to form regularly ordered structures.[5,6] These well-ordered ionic moieties are expected to work as efficient cation carriers and scaffolds for ordering cations. These materials, which comprise closely assembled ionic species, can exhibit interesting optical and magnetic properties. Thus, new molecular designs for preparing thermally stable LCs composed of ionic species are needed to produce advanced functional materials.

The concept of supported IL phases (SILPs) has been recently proposed. Several materials based on SILPs have exhibited important characteristics such as high ion conductivity and compatibility with organic reaction media; these materials have been used as templates for the formation of nanostructures.[1] Silica supports improve the thermal stability of LCs.[7,8] Carmichael *et al.*[9] have synthesized and explored silicon wafer-assisted SILP materials. They created layers with thicknesses between 10 and 21 nm of an ionic LC with $[C_{18}C_1Im][PF_6]$ on the planar wafer surface and found that the ionic LC formed a mesophase. Inspired by their work, Wasserscheid *et al.*[7] fabricated SILP materials using silicon nanoparticles and used them as supports for preparing mesoporous structures that could act as effective gas-phase catalysts.[8] To construct advanced materials based on the concept of SILP materials, their properties must be fine-tuned according to preprogramed designs at the molecular level. A wide variety of polyhedral oligomeric silsesquioxane (POSS)-based functional materials have been developed using ionic species.[10–24] We recently reported the synthesis of POSS-based ILs, and we investigated their thermal properties.[25,26] By tethering multiple ion pairs composed of imidazolium cations and carboxylates to the vertices of POSS cores or by simply adding POSS molecules with acid groups, the melting temperatures of the ion pairs decreased and their thermal stabilities increased.[25–28] In the crystalline state, the POSS core can isolate each ion pair. As a result, the intermolecular interactions are reduced, and thus the melting temperatures are decreased. In the liquid state, the ion pairs are distributed in a spherical conformation as a result of their tethering to the POSS core. Therefore, their molecular symmetry can be improved and their thermal stability can be enhanced. Finally, we reported on the synthesis of room temperature ILs using POSS.[25] Our interests have shifted, and we would like to exploit the thermal properties of POSS for realizing optical materials. In particular, we aim to construct unique optical materials based on SILP materials that utilize the structural features of POSS.

Herein, we report the extension of the temperature range of the LC phase by the POSS core. Ion pairs of carboxylate and imidazolium with various alkyl chain lengths were prepared, and the influence of the length of the alkyl chains and their tethering to the POSS core on the thermal properties of the ion pairs was investigated. Initially, the ion salts with the octadecyl alkyl chains at the imidazolium moiety exhibited LC phases. Significantly, the isotropic phase of the obtained POSS ion salts was not detected until decomposition occurred during the heating process. In other words, the temperature range of the LC phase was extended by the POSS core. In contrast, the ion salts that were not tethered to a POSS core showed a clearance point during heating. We propose that the highly symmetric structure of the POSS

Department of Polymer Chemistry, Graduate School of Engineering, Kyoto University, Kyoto, Japan
Correspondence: Professor Y Chujo or DR K Tanaka, Department of Polymer Chemistry, Graduate School of Engineering, Kyoto University, Katsura, Nishikyo-ku, Kyoto 615-8510, Japan.
E-mail: chujo@chujo.synchem.kyoto-u.ac.jp or kazuo123@chujo.synchem.kyoto-u.ac.jp
Received 24 December 2014; revised 15 February 2015; accepted 22 February 2015

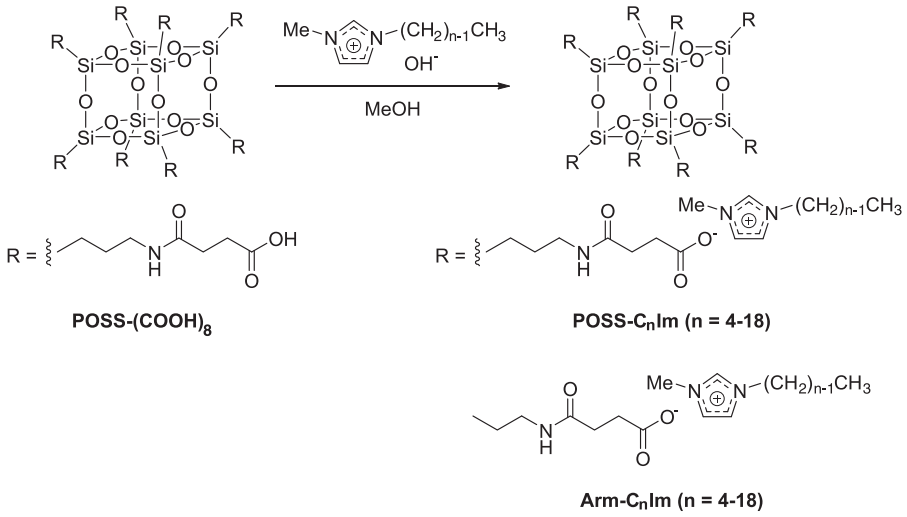

Scheme 1 Chemical structures and synthetic scheme for preparing the ion salts used in this study.

core should contribute not only to the suppression of the molecular motion of the ion salts but also to the formation of regular structures. To the best of our knowledge, this is the first time that a significant enhancement of LC formation has been detected using the structural characteristics of a molecular cube that imparts the IL crystals with unique thermal stabilities.

EXPERIMENTAL PROCEDURE

General procedure for the preparation of ILs

The desired equivalent moles of the bromide anion to the carboxyl groups were converted into the hydroxylic form using an anion exchange resin (Amberlite–IRA400, Sigma-Aldrich Inc., St Louis, MO, USA) in water and neutralized by suspension in methanol (2 l). The aqueous solution was concentrated using a rotary evaporator, and the residual liquid was freeze-dehydrated to give the white solid. The solid was dried *in vacuo* and stored in a glove box.

Differential scanning calorimetry (DSC)

DSC thermograms were produced on a SII DSC 6220 instrument (Seiko Instruments Inc., Chiba, Japan) using ~10 mg of sample. The sample on the aluminum open pan was cooled to –130 °C at the rate of 10 °C min^{-1} under flowing nitrogen (30 ml min^{-1}) and then heated from –130 to 80 °C at the same rate. The glass transition (T_g) and melting temperatures (T_m) were determined as the onset of the second curves to eliminate heat history. The fusion enthalpies (ΔH_{fus}) were calculated from the areas of the endothermic peaks in the first cycle with the completely crystallized samples soaked in liquid nitrogen before measurement. To collect the transition temperatures of the mesophases, the measurements were monitored at a rate of 5 °C min^{-1}. The transition temperatures ($T_{lc\text{-}iso}$) were evaluated from the second heating curves.

Thermogravimetric analysis (TGA)

TGA was performed on an EXSTAR TG/DTA6220 (Seiko Instrument, Inc.) at a heating rate of 10 °C min^{-1} up to a temperature 900 °C under flowing nitrogen (200 ml min^{-1}). Residual water was removed by keeping the platinum pan at 110 °C for 1 h before the curve profiling was completed. The decomposition temperatures (T_d) were determined from the onset of the weight loss.

RESULTS AND DISCUSSION

Smaller fusion entropies were obtained during the melting process for POSS-tethered ion salts than for ion salts without POSS.[25,26] Thus, it is likely that the molecular distribution of the ion pairs that are tethered to the POSS core in the crystals remain the same after melting, meaning that a star-shaped structure might be maintained before and after melting. Based on these presumptions, we aimed to align the POSS molecules to form regular structures in the liquid phase. By elongating the alkyl chains of the imidazolium cation, the hydrophobic interactions among the ion pair moieties should be enhanced, leading to the formation of well-aligned, high-dimensional structures in the POSS-based ILs. A series of POSS-tethered ion pairs with longer imidazolium cation alkyl chains were synthesized (Scheme 1; the detailed procedures and characterization data are shown in the Supporting Information). During anion exchange, the 1-alkyl-3-methylimidazolium bromides were transformed to the hydroxide form, and the desired products were prepared via neutralization with POSS-$(COOH)_8$.[25] After lyophilization, the products obtained were either colorless and transparent liquids or white solids. To prohibit coloration, all procedures were carried out without heating. We also prepared the ion pair Arm-C_nIm and used it to evaluate the effect of the connection to the POSS core on the thermal properties of the materials.

The ^{29}Si nuclear magnetic resonance spectra of all of the samples containing the POSS moiety exhibited a single peak at ~66 p.p.m. that was assigned to the T_8 POSS structure.[25,26] These data indicate that the POSS cage is not significantly degraded in the final products. The integration of the peaks in the ^{1}H nuclear magnetic resonance spectra indicates the formation of 1:8 ion pairs of POSS-$(COOH)_8$ and imidazolium cation. All samples were stored in a glove box under an argon atmosphere, and the water abundance was held below 1.5 wt. % as determined by the Karl Fischer method. The concentration of residual bromide ion was lower than the detectable level as determined by elemental analysis. Therefore, we concluded that all products were sufficiently pure.

Initially, the thermal stability of the synthetic compounds against pyrolysis was investigated using TGA. The T_d, evaluated from the onsets of the TGA profiles, are summarized in Figure 1a (values are listed in Table S1 in the Supporting Information). It was found that the T_d values for the POSS-C_nIm samples were higher than those for the Arm-C_nIm samples with the same alkyl chain length. When the length of the alkyl chain of the imidazolium cation was increased, the T_d values of the POSS-C_nIm samples gradually decreased. Conversely, those of the Arm-C_nIm samples remained constant. The decomposition fragment of the molecule can be determined by evaluating the vertical bars in these profiles (from the weight loss to the molecular weight).[25,26] As a result, the decomposition process was

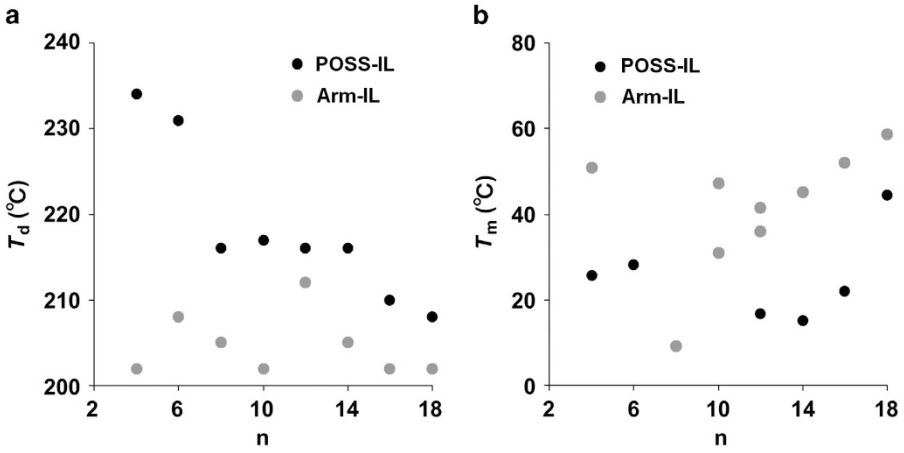

Figure 1 Decomposition (**a**) and melting (**b**) temperatures of the ion salts with variable imidazolium cation alkyl chain lengths. POSS, polyhedral oligomeric silsesquioxane; T_d, decomposition temperature; T_m, melting temperature.

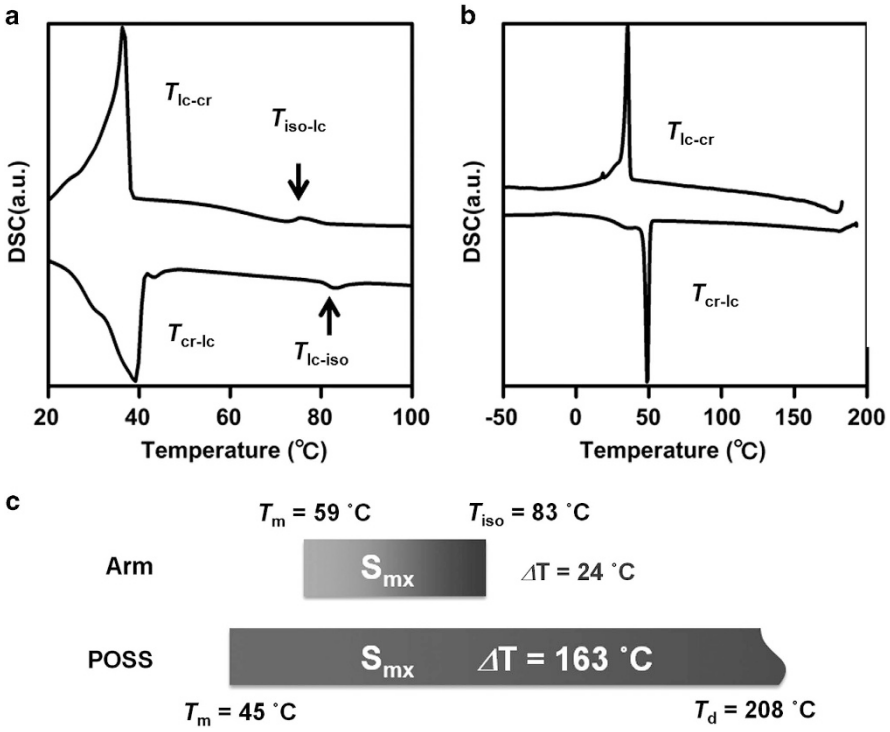

Figure 2 Differential scanning calorimetry (DSC) profiles of (**a**) Arm-C_{18}Im and (**b**) POSS-C_{18}Im. (**c**) Summary of the phase transition temperatures of the ion salts, including the T_ms, as shown in Figure 1. POSS, polyhedral oligomeric silsesquioxane; T_d, decomposition temperature; T_m, melting temperature.

explored. According to these decomposition mechanisms, the degradation should occur at the imidazolium ion pairs. These results indicate the stabilizing effect of the POSS core on the T_d regardless of the alkyl chain length of the imidazolium moiety. In particular, the T_d values were higher for the POSS salts with long alkyl chains, in which the POSS core did not greatly influence the molecular stabilization, than for the Arm salts. Regular structures, originating from the cubic core, might be formed; these structures may increase the stability of the system by limiting the thermal motion of the remote alkyl chains.

The T_m was determined from the peak top in the second cycle of DSC analysis (heating rate = 10 °C min^{-1}, Figure 1b (values are listed in Table S2 in the Supporting Information)). Most samples exhibited endothermic peaks below 100 °C. Therefore, they were classified as ILs.[29] The POSS moiety can decrease the T_m values of the ion salts; this phenomenon can be seen by comparing the T_m values of ILs with the same alkyl chain lengths (POSS-C_nIm and Arm-C_nIm). These data can be explained by noting that the cubic core can inhibit molecular interactions between the ion salts.[25,26] In particular, for the POSS-C_nIm samples, the alkyl chain length did not significantly influence the T_m values (for below $n = 14$). POSS-C_{16}Im can be categorized as a room temperature IL (an IL with a T_m below 25 °C). Conversely, Arm-C_nIm (alkyl length, $n = 8$) showed the lowest melting temperature, and the introduction of a longer alkyl chain (more than $n = 10$) caused the T_m values to significantly increase. In general, such T_m

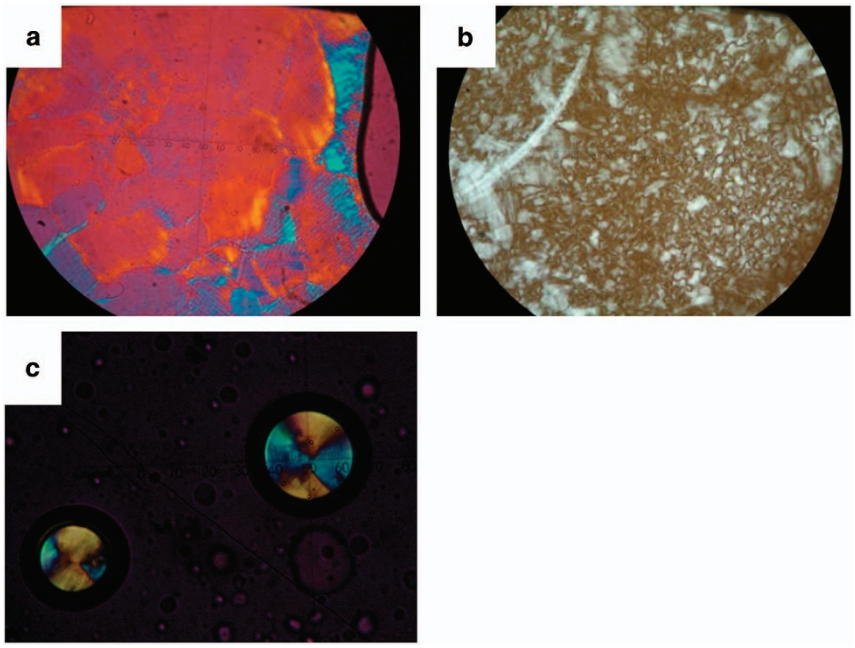

Figure 3 Polarized optical microscopy (POM) textures of POSS-C_{18}Im samples at (**a**) 40 °C and (**b**) 100 °C and (**c**) an Arm-C_{18}Im sample at 40 °C during the first cooling process. POSS, polyhedral oligomeric silsesquioxane.

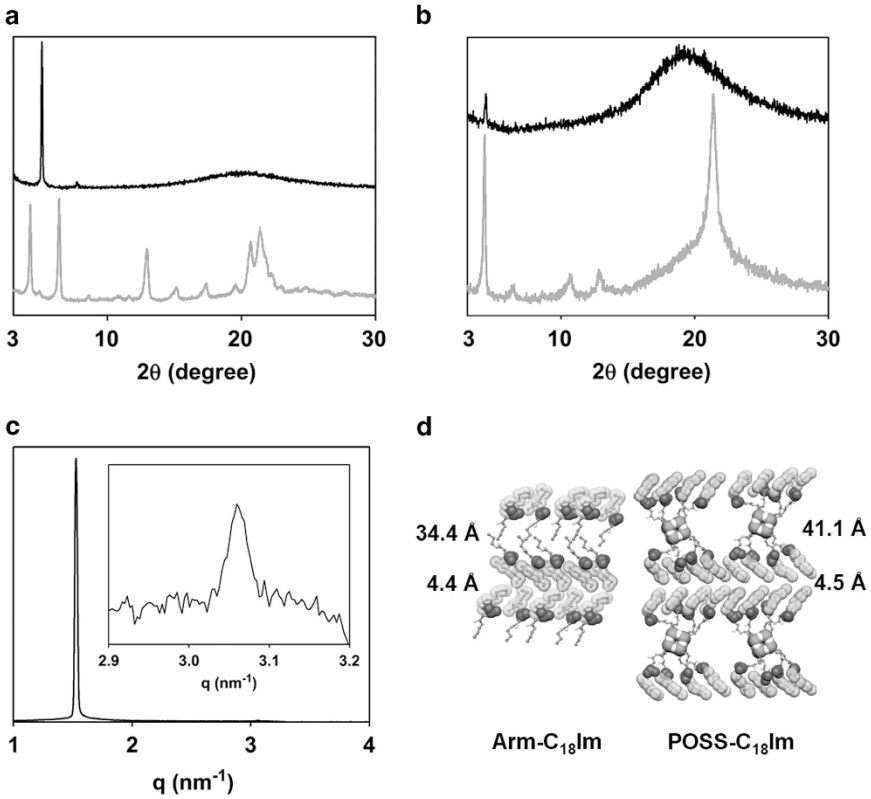

Figure 4 Variable temperature powder X-ray diffraction (VT-PXRD) patterns of (**a**) Arm-C_{18}Im at 60 °C (black line) and 30 °C (gray line) and (**b**) POSS-C_{18}Im at 100 °C (black line) and 30 °C (gray line). (**c**) One-dimensional small-angle X-ray scattering (1D SAXS) patterns of POSS-C_{18}Im at 100 °C. (**d**) Proposed model of the liquid crystal structures. POSS, polyhedral oligomeric silsesquioxane.

dependencies have been observed in other types of ILs, and the lowest melting temperature was typically found for systems with alkyl chain lengths between $n=2$ and $n=8$.[30] The T_m data, along with the TGA results, imply that the POSS core could significantly dominate the distributions of ion pairs. Thereby, the formation of the most thermally stable structure should be inhibited. Notably, the T_m value of the POSS salt with the C_{18} alkyl chains, where the POSS core does not likely influence the system to the same extent, was still lower than

that of the Arm salt. This result implies that regular structures are formed. T_m values could not be reliably obtained for POSS-C_8Im and POSS-C_{10}Im because of their extremely poor crystallinities; unstable metastable states also exist in these structures.

The fusion enthalpies and entropies (ΔH_{fus} and ΔS_{fus}) for the single imidazolium molecule with POSS-C_{18}Im and Arm-C_{18}Im were evaluated from the areas of the endothermic peaks observed in the DSC profiles. Interestingly, smaller thermodynamic parameters ($\Delta H_{fus} = 30\ kJ\ mol^{-1}$, $\Delta S_{fus} = 96\ J\ mol^{-1}\ K^{-1}$) were obtained for the POSS-C_{18}Im sample than for the Arm-C_{18}Im sample ($\Delta H_{fus} = 65\ kJ\ mol^{-1}$, $\Delta S_{fus} = 196\ J\ mol^{-1}\ K^{-1}$). These thermal data are typical for POSS ILs.[25,26] The cubic silica core can isolate each ion pair. In addition, the star-shaped structure of the whole molecules comprising the POSS ILs should make interactions among ion pairs unfavorable. Smaller ΔH_{fus} values were observed, leading to decreases in the T_m. Moreover, the star-shaped structure likely reduces the conformational variety of the ion pairs because of its high symmetry even in the liquid phase. Thus, thermal stability toward pyrolysis can be acquired. Such thermal characteristics, which originate from the POSS core, can be obtained for the C_{18}Im salts. It is likely that the regular structure transmits the effect of the POSS core through the material.

Using DSC analysis, the phase transition behaviors of the salts containing C_{18}Im were investigated (Figure 2). To collect a high resolution profile, the temperature was changed slowly ($5\ °C\ min^{-1}$). Although the endothermic peak associated with the melting of the Arm-C_{18}Im samples was unclear, an endothermic transition was observed at 83 °C ($T_{lc\text{-}iso}$) after melting (Figure 2a). In contrast, the POSS-C_{18}Im samples presented a clear endothermic transition at 45 °C that could be attributed to melting, and these samples did not show any other transitions until the decomposition temperature (Figure 2b). As summarized in Figure 2c, and in light of the T_ms included in Figure 1, it is likely that the POSS-C_{18}Im sample maintained its mesophase until the decomposition temperature and showed mesophase stability over a much wider temperature range ($\Delta T = 163$ °C) than the Arm-C_{18}Im sample ($\Delta T = 24$ °C). Therefore, the connection of the ion salts to the POSS core greatly enhances the mesophase stability of ILs (higher mesophase stability, lower melting temperature). Polarized optical microscopy was performed on the samples containing C_{18}Im (Figure 3). Arm-C_{18}Im exhibited a focal-conic fan-like texture at 40 °C. Conversely, POSS-C_{18}Im showed a mesophase of broken or small focal-conic fan-like texture. In particular, the mesophase of POSS-C_{18}Im was maintained even at 100 °C. These results indicate that both Arm-C_{18}Im and POSS-C_{18}Im formed smectic mesophases. In particular, because POSS-C_{18}Im shows higher thermal stability compared with Arm-C_{18}Im, it is likely that the connection of the ion salts to POSS can extend the temperature region in which the samples act as thermotropic LCs.

Variable temperature powder X-ray diffraction experiments were also executed to estimate the structures of the LCs (rate = $1\ °C\ min^{-1}$, Figure 4). In the Arm-C_{18}Im mesophase, at 60 °C, two pairs of diffraction peaks were observed (at 5.11° and 7.70°); these peaks were attributed to the (02) and (03) peaks (d-spacing = 34.4 Å) derived from the smectic layer distance (Figure 4a). Moreover, a wide-angle, broad halo peak was also observed at ~20.0° (d-spacing = 4.4 Å). This peak could be attributed to the molten alkyl chains. In contrast, in the POSS-C_{18}Im mesophase, one diffraction peak was observed at 4.30°, and a broad halo was observed at ~19.7° (d-spacing = 4.5 Å) at 100 °C (Figure 4b). In small-angle X-ray scattering experiments (Figure 4c), two pairs of diffraction peaks (at q = 1.528 and $3.06\ nm^{-1}$ (d-spacing = 41.1 Å)) were observed; these peaks were derived from the smectic layer distance. These values are consistent with the X-ray diffraction peaks attributed to the (02) diffraction. The extension of the d-spacing determined from the (02) diffraction can be explained by considering the size of the POSS core. By inserting the silica cube (~5 Å in diameter), the layer distance was expanded (Figure 4d). Thus, a larger value was obtained.

CONCLUSION

POSS-based imidazolium salts with various alkyl chain lengths possessed melting temperatures below 100 °C and turned out to be ILs. For butyl to octadecyl alkyl chains, the POSS ion salts showed higher thermal stabilities and lower melting temperatures than the corresponding Arm ion salts. The properties of the POSS-C_{18}Im samples can be explained by considering the rigid cubic structure and the molecular shape of the POSS core. During the melting process, the POSS core reduces molecular interactions between the ion pairs. After melting, the POSS core induces regular structures in the ion salts, even in the liquid phase. Thus, it was demonstrated that POSS-C_{18}Im samples showed much higher mesophase stabilities. Thermally stable thermotropic IL crystals are useful in modern electronic devices. These findings should have important implications for the preparation of the new series of IL crystals involving nanostructures.

CONFLICT OF INTEREST

The authors declare no conflict of interest.

ACKNOWLEDGEMENTS

We thank Professor Susumu Kitagawa and Dr Satoshi Horike (Kyoto University) for the use of the VT-XRD instrument and Professor Hirokazu Hasegawa and Dr Kenji Saijo (Kyoto University) for the use of the SAXS instrument. We acknowledge Professor Kazuo Akagi and Dr Munju Goh (Kyoto University) for their advice concerning the structural analysis of the liquid crystals. This work was partially supported by a Grant-in-Aid for Scientific Research on Innovative Areas 'New Polymeric Materials Based on Element-Blocks (No.2401)' (25102521) from The Ministry of Education, Culture, Sports, Science, and Technology (Japan).

1 Binnemans, K. Ionic liquid crystals. *Chem. Rev.* **105**, 4148–4204 (2005).
2 Axenov, K. & Laschat, S. Thermotropic ionic liquid crystals. *Materials* **4**, 206–259 (2011).
3 Goh, M., Park, J., Han, Y., Ahn, S. & Akagi, K. Chirality transfer from atropisomeric chiral inducers to nematic and smectic liquid crystals – synthesis and characterization of di- and tetra-substituted axially chiral binaphthyl derivatives. *J. Mater. Chem.* **22**, 25011–25018 (2012).
4 Wezenberg, S. J., Ferroni, F., Pieraccini, S., Schweizer, W. B., Ferrarini, A., Spada, G. P. & Diederich, F. Effective cholesteric liquid crystal inducers based on axially chiral alleno-acetylenes. *RSC Adv.* **3**, 22845–22848 (2013).
5 Yoshio, M., Mukai, T., Ohno, H. & Kato, T. One-dimensional ion transport in self-organized columnar ionic liquids. *J. Am. Chem. Soc.* **126**, 994–995 (2004).
6 Yoshio, M., Kagata, T., Hoshino, K., Mukai, T., Ohno, H. & Kato, T. One-dimensional ion-conductive polymer films: alignment and fixation of ionic channels formed by self-organization of polymerizable columnar liquid crystals. *J. Am. Chem. Soc.* **128**, 5570–5577 (2006).
7 Kohler, F. T.U., Morain, B., Weiss, A., Laurin, M., Libuda, J., Wagner, V., Melcher, B. U., Wang, X., Meyer, K. & Wasserscheid, P. Surface-functionalized ionic liquid crystal-supported ionic liquid phase materials: ionic liquid crystals in mesopores. *ChemPhysChem* **12**, 3539–3546 (2011).
8 Shi, F., Zhang, Q., Li, D. & Deng, Y. Silica-gel-confined ionic liquids: a new attempt for the development of supported nanoliquid catalysis. *Chem. Eur. J.* **12**, 5279–5288 (2005).
9 Carmichael, A. J., Hardacre, C., Holbrey, J. D., Nieuwenhuyzen, M. & Seddon, K. R. Molecular layering and local order in thin films of 1-alkyl-3-methylimidazolium ionic liquids using X-ray reflectivity. *Mol. Phys.* **99**, 795–800 (2001).
10 Tanaka, K. & Chujo, Y. Chemicals-inspired biomaterials; developing biomaterials inspired by material science based on POSS. *Bull. Chem. Soc. Jpn* **86**, 1231–1239 (2013).
11 Kaneko, Y., Toyodome, H., Mizumo, T., Shikinaka, K. & Iyi, N. Preparation of a sulfo-group-containing rod-like polysilsesquioxane with a hexagonally stacked structure and its proton conductivity. *Chem. Eur. J.* **20**, 9394–9399 (2014).

12 Toyodome, H., Higo, Y., Sasai, R., Kurawaki, J. & Kaneko, Y. Behavior of chiral induction from polysilsesquioxanes bearing chiral and ammonium groups to anionic pyrene derivatives. *J. Nanosci. Nanotechnol.* **13**, 3074–3078 (2013).
13 Yamamoto, E., Kitahara, M., Tsumura, T. & Kuroda, K. Preparation of size-controlled monodisperse colloidal mesoporous silica nanoparticles and fabrication of colloidal crystals. *Chem. Mater.* **26**, 2927–2933 (2014).
14 Nakato, T., Yamashita, Y., Mouria, E. & Kuroda, K. Multiphase coexistence and destabilization of liquid crystalline binary nanosheet colloids of titanate and clay. *Soft Mater.* **10**, 3161–3165 (2014).
15 Kuroda, K., Shimojima, A., Kawahara, K., Wakabayashi, R., Tamura, Y., Asakura, Y. & Kitahara, M. Utilization of alkoxysilyl groups for the creation of structurally controlled siloxane-based nanomaterials. *Chem. Mater.* **26**, 211–220 (2014).
16 Jovanovski, V., Orel, B., Ješe, R., Vuk, A.Š., Mali, G., Hočevar, S. B., Grdadolnik, J., Stathatos, E. & Lianos, P. Novel polysilsesquioxane – I-/I3- ionic electrolyte for dye-sensitized photoelectrochemical cells. *J. Phys. Chem. B* **109**, 14387–14395 (2005).
17 Jovanovski, V., Orel, B., Ješe, R., Mali, G., Stathatos, E. & Lianos, P. Degradation of aqueous methyl tert-butyl ether by photochemical, biological, and their combined processes. *Int. J. Photoenergy* **8**, 1–8 (2006).
18 Vuk, A.Š., Jovanovski, V., Pollet-Villard, A., Jerman, I. & Orel, B. Imidazolium-based ionic liquid derivatives for application in electrochromatic devices. *Sol. Energy Mater. Sol. Cells* **92**, 126–135 (2008).
19 Subianto, S., Mistry, M. K., Choudhury, N. R., Dutta, N. K. & Knott, R. Composite polymer electrolyte containing ionic liquid and functionalized polyhedral oligomeric silsesquioxanes for anhydrous PEM applications. *ACS Appl. Mater. Interfaces* **6**, 1173–1182 (2009).
20 Naka, K., Shinke, R., Yamada, M., Djouadi Belkada, F., Aijo, Y., Irie, Y., Ram Shankar, S., Sai Smaran, K., Matsumi, N., Tomita, S. & Sakurai, S. Synthesis of imidazolium salt-terminated poly(amidoamine)-typed POSS-core dendrimers and their solution and bulk properties. *Polym. J.* **46**, 42–51 (2014).
21 Naka, K., Masuoka, S., Shinke, R. & Yamada, M. Synthesis of first and second generation imidazole-terminated POSS-core dendrimers and their pH responsive and coordination properties. *Polym. J.* **44**, 353–359 (2012).
22 Ishii, T., Mizumo, T. & Kaneko, Y. Facile preparation of ionic liquid containing silsesquioxane framework. *Bull. Chem. Soc. Jpn* **87**, 155–159 (2014).
23 Tanaka, K. & Chujo, Y. Unique properties of amphiphilic POSS and their applications. *Polym. J.* **45**, 247–254 (2013).
24 Tanaka, K. & Chujo, Y. Advanced functional materials based on polyhedral oligomeric silsesquioxane (POSS). *J. Mater. Chem.* **22**, 1733–1746 (2012).
25 Tanaka, K., Ishiguro, F. & Chujo, Y. POSS ionic liquid. *J. Am. Chem. Soc.* **132**, 17649–17651 (2010).
26 Tanaka, K., Ishiguro, F. & Chujo, Y. Thermodynamic study of POSS-based ionic liquids with various numbers of ion pairs. *Polym. J.* **43**, 708–713 (2011).
27 Jeon, J.-H., Tanaka, K. & Chujo, Y. POSS fillers for modulating thermal properties of ionic liquids. *RSC Adv.* **3**, 2422–2427 (2013).
28 Jeon, J.-H., Tanaka, K. & Chujo, Y. Synthesis of sulfonic acid-containing POSS and its filler effects for enhancing thermal stabilities and lowering melting temperatures of ionic liquids. *J. Mater. Chem. A* **2**, 624–630 (2014).
29 Rogers, R. D. & Seddon, K. R. Ionic liquids–solvents of the future? *Science* **302**, 792–793 (2003).
30 Holbrey, J. D. & Seddon, K. R. The phase behaviour of 1-alkyl-3-methylimidazolium tetrafluoroborates; ionic liquids and ionic liquid crystals. *J. Chem. Soc. Dalton Trans.* 2133–2139 (1999).

Supplementary Information accompanies the paper on the NPG Asia Materials website (http://www.nature.com/am)